

RESEARCH

Open Access



# A multi-analytical approach to identify ancient pigments used in pottery towers excavated from the Han Dynasty tombs

InHee Go<sup>1</sup>, Jingqi Wen<sup>1,2</sup>, Xiang He<sup>1</sup>, Naitao Liu<sup>3</sup> and Hong Guo<sup>1\*</sup>

## Abstract

In 2013, several tombs were discovered and excavated in Southeastern Beijing, China, yielding various burial products. Among these were pottery towers, a representative artifact of the Han Dynasty rarely found in the area. Many studies on architectural aspects, such as construction type and construction situation, have been conducted based on the excavated pottery towers, but only a few have examined their raw materials or pigments. In this study, black, white, and red pigments were identified as carbon black, calcite, and cinnabar, respectively, through a multi-analysis approach. The manufacturing method of the pigment was established based on the crystal form and particle size of the pigment, by factoring in the pigment characteristics, which cannot be distinguished by component analysis and crystal structure analysis. We recommend that a continuous database be prepared and used in the future, not only for an interpretation of ancient pigments but also to identify the factors to be considered (physical characteristics, such as pigment particle size among others) when estimating the manufacturing process and conservation treatment.

**Keywords** Ancient pigment, Pottery tower, Pigment particle shape, Daqu tomb, Han Dynasty

## Introduction

Thirty-two tombs were excavated in Daqu town, Daxing District, Beijing, China (Fig. 1A), and various burial products (colored pottery towers, cups, lanterns, etc.) were found. Beijing belonged to the Youzhou [幽州] region in the Later Han Dynasty (CE 25–220) and, according to archaeological clues, such as the type of tomb (brick tomb, see Fig. 1B) and the type of burial products (see

Fig. 1C), the tombs were dated from the Later Han period [1].

Numerous colored pottery towers were found in the Hebei, Jiangsu, and, in particular, Henan and Shaanxi provinces. Since the first such discovery was made in Beijing, these artifacts have been attracting great attention, due to their size of up to 2 m, their quantity is large, and the relatively good condition of the funeral products. The Han Dynasty was a time of great political, economic, and cultural development for China; it was also a technologically mature period where the arts, including architectural culture, flourished. Extant literature maintains several records of pottery towers from the Han Dynasty [2]. Cultural artifacts found from archaeological excavations of tombs have been accumulating over many years. Research has made significant progress in understanding the architectural style of the Later Han Dynasty based on these pottery towers, which are miniature replicas of buildings of that time [2, 3]. The insights derived from

\*Correspondence:

Hong Guo  
guohong54321@163.com

<sup>1</sup> Institute for Cultural Heritage and History of Science and Technology, University of Science and Technology Beijing, Beijing, 100083, People's Republic of China

<sup>2</sup> National Centre for Archaeology, Beijing, 100013, People's Republic of China

<sup>3</sup> Beijing Archaeology Historic Site Museum, Beijing, 100160, People's Republic of China



© The Author(s) 2023. **Open Access** This article is licensed under a Creative Commons Attribution 4.0 International License, which permits use, sharing, adaptation, distribution and reproduction in any medium or format, as long as you give appropriate credit to the original author(s) and the source, provide a link to the Creative Commons licence, and indicate if changes were made. The images or other third party material in this article are included in the article's Creative Commons licence, unless indicated otherwise in a credit line to the material. If material is not included in the article's Creative Commons licence and your intended use is not permitted by statutory regulation or exceeds the permitted use, you will need to obtain permission directly from the copyright holder. To view a copy of this licence, visit <http://creativecommons.org/licenses/by/4.0/>. The Creative Commons Public Domain Dedication waiver (<http://creativecommons.org/publicdomain/zero/1.0/>) applies to the data made available in this article, unless otherwise stated in a credit line to the data.

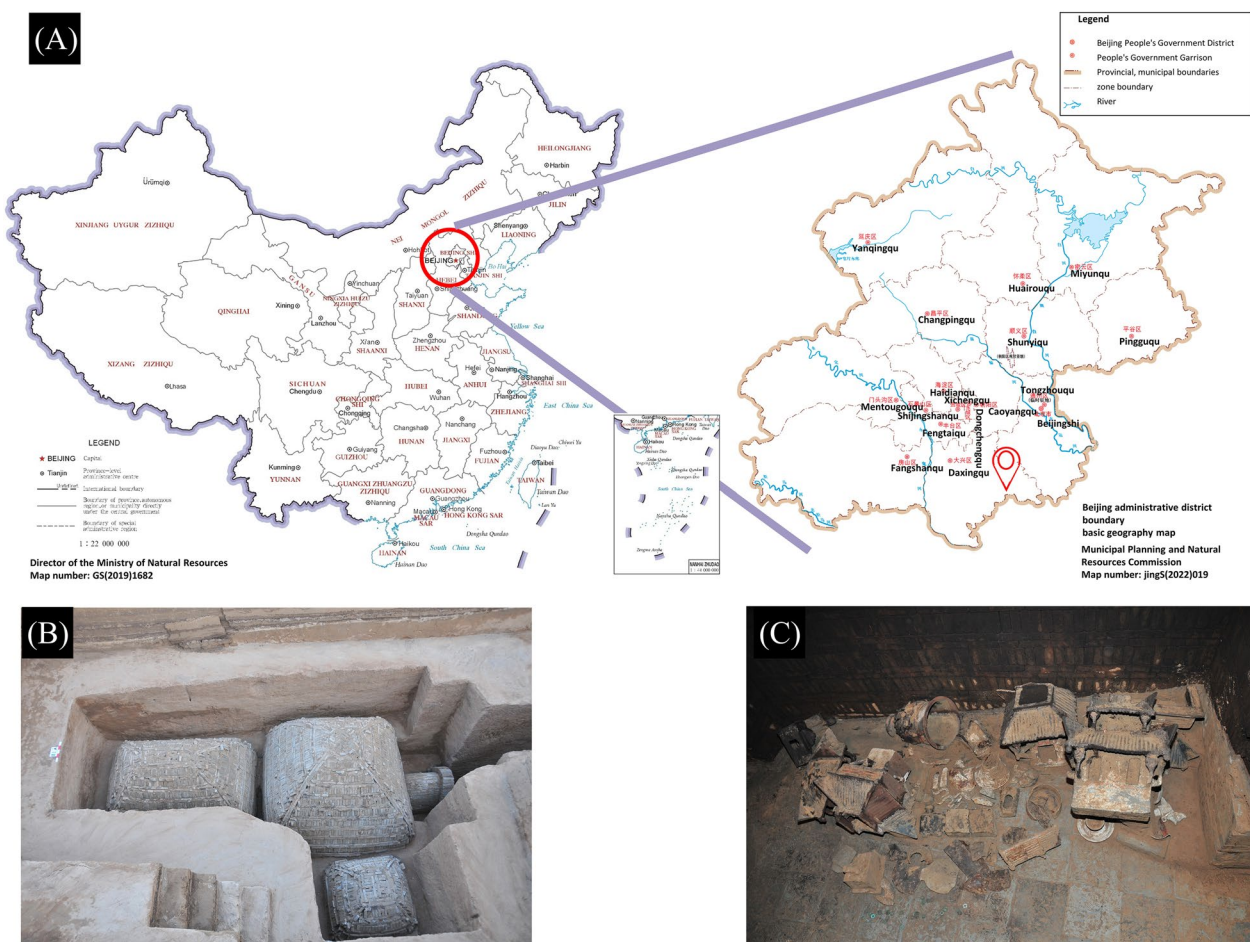


**Fig. 1** The pottery towers excavation area in Daxing District, Han Dynasty (**A** map of the excavation area; **B** brick tomb; **C** excavated artifacts)

such studies have enriched several research fields including archaeology, architecture, culture, and art. However, the technological aspects of the towers have been insufficiently analyzed.

Chinese old literature (such as *Shuowen Jiezi* [说文解字] and *Qimin Yaoshu* [齐民要术]) mentions the manufacturing method, characteristics, and usage of diverse pigments (ink stick, cinnabar, etc.). However, such references date primarily from the Ming and Qing dynasties; the earliest period was the *Shuowen Jiezi* [说文解字] in the Eastern Han Dynasty. Based on the names of the pigments mentioned in the Eastern Han Dynasty, we can conclude these were produced and used from an even earlier era.

According to previous studies, cinnabar was the most used red color in tomb murals in the Han Dynasty, and carbon black and graphite were the colors most commonly used to paint anything black. In addition, chalk, lead powder, and feldspar were expressed in white, and the material is relatively abundant compared to other pigments. The differences in the materials used are

reportedly due to the influence of the selection of raw materials that were relatively easy to obtain in the deposit area, and because pigment milling and manufacturing in the Han Dynasty were well-developed [4–6].

Therefore, in this study, multiple analytical methods such as microscopy, Raman spectroscopy, and scanning electron microscopy/energy dispersive spectroscopy (SEM–EDS), were used to identify the constituents of the pigments, as well as to present an analysis approach suitable for each type of pigment. In addition, the pigment manufacturing process was estimated based on the crystal shape and particle size, and the characteristics of the pigment, which cannot be distinguished by component analysis and crystal structure analysis, were factored in.

## Materials and methods

### Materials

The samples used in this study were carefully collected from different pottery tower fragments (Fig. 2) excavated in Daqu. These were in black, white, and red colors. A



**Fig. 2** Pottery towers excavated from the tomb in the Han Dynasty (sample numbers from L to R: DAM11-37, DAM11-38, DAM1-30, DAM15-71)

sample for cross-section observation was embedded in a certain ratio of two-component epoxy resin (Epoxy-MountKit: 145-10005, High Tech Products, Inc.), which was then ground and polished [7].

### Analysis methods

#### Optical microscopy

A Keyence VHX-6000 3D digital microscope system (manufactured in Japan) with ultra depth of field was used to perform cross-section and surface observations of two types of samples (cross-section and sample surfaces) at magnifications ranging from 50 to 2000 times.

#### Chromaticity

A 3nh NH310 portable colorimeter (manufactured in China) was used to express CIE  $L^*$ ,  $a^*$ , and  $b^*$  to quantify the brightness and chroma of the pigment samples. The measuring aperture used was 8 mm. The locations measured for chromaticity measurement were parts representing white, black, and red. Measurements were made three times, and the average value was used; it is marked with the round red line in Fig. 3.

#### Scanning electron microscopy/energy dispersive spectroscopy (SEM-EDS)

SEM-EDS (Hitachi, SU8100, Japan) was used for the micro-structuring and component analysis of microscopic areas of the samples. The sample was fixated with carbon tape and coated with platinum (Pt). The component content of the pigment was obtained through mapping analysis.

#### Portable X-ray fluorescence (p-XRF)

Qualitative and quantitative analyses of major elements in the pigment samples were carried out by Niton series XRF XL3t (Thermo Fisher, USA), with the following measuring conditions soil mode. The measurement locations are indicated by red circles in Fig. 3, and the data

were measured three times in the same spot and the average values were used.

#### Raman spectroscopy

The pigments were qualitatively analyzed using Raman spectrometers (Nicolet Almega XR, Thermo Fisher, USA) and a microscope (Olympus BX-41). The laser energy was about 12.5 mW, the slit width 100  $\mu\text{m}$ , the objective lens used for the test magnified 10–100 times, and the spot size was 1  $\mu\text{m}$ . As for the laser source, 532 nm, 638 nm, and 785 nm wavelengths were alternately used and the experiments conducted under conditions to obtain suitable spectra.

#### Polarized-light microscope

The polarized-light microscope used in the experiment was Leica's DM2700p (manufactured in Germany). As a pre-treatment step, the pigment sample was positioned at the center of a microscope glass slide and sealed with a cover glass slip. A small amount of distilled water was introduced between the glass slide and the cover glass slip, and gentle pressure was applied to secure the cover glass slip in place.

## Results and discussion

### Pigment characteristics

#### Color difference analysis

Quantifying the color of a paint layer and identifying objective color values are important because the color in a pigment depends on its particle size. Unlike modern pigments, ancient ones were not composed of uniformly sized particles. Therefore, when repairing and restoring with the same material, the color may have varied depending on the size and distribution of the pigment particles.

The average L values of the pigments were 75.64, 36.49, and 54.83 for white, black, and red pigments,

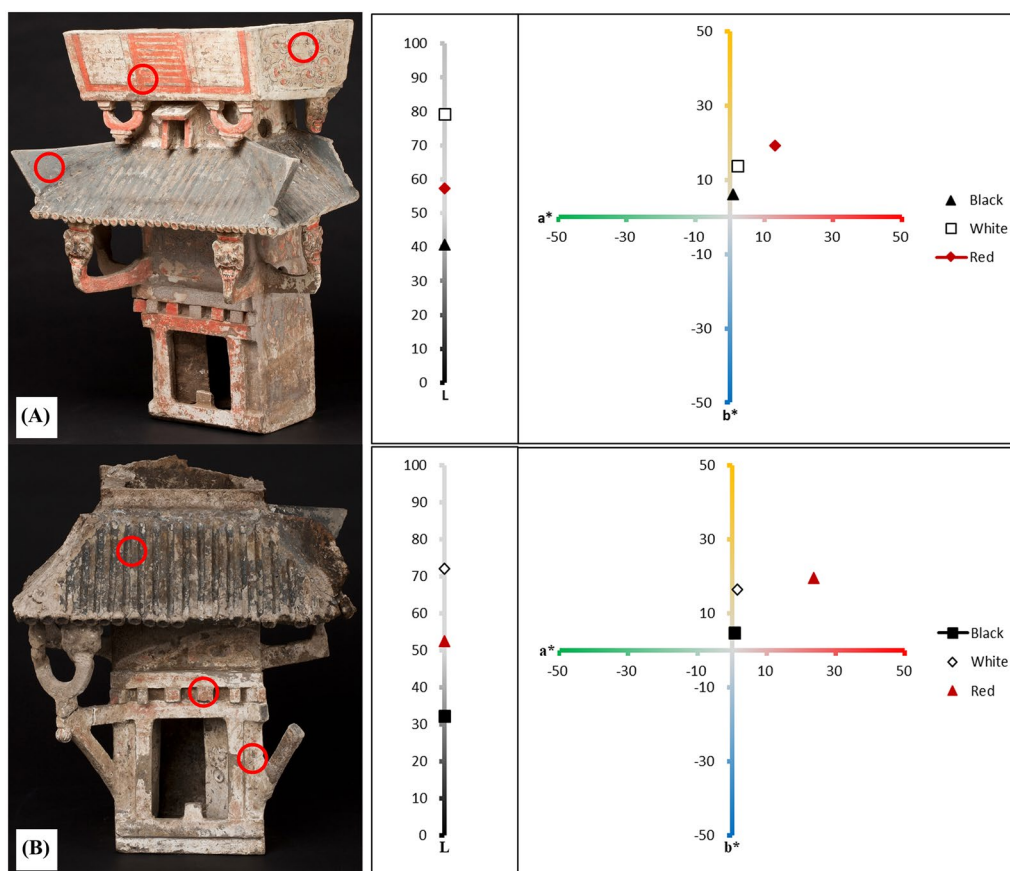


**Fig. 3** Chromaticity diagram of three types of pigments (**A** DAM11-37, **B** DAM11-30)

respectively. The mean values of  $a^*$ , representing the scale of green ( $-a^*$ ) and red ( $+a^*$ ), were 1.80, 0.73, and 18.37. The mean values of  $b^*$ , indicating the measure of blue ( $-b^*$ ) and yellow ( $+b^*$ ) scales, were 15.12, 5.45, and 19.41. Of particular interest was the white pigment, which showed a relatively high  $L^*$  value; the red one had a high value representing the scale of green ( $-a^*$ ) and red ( $+a^*$ ), and the black one had the lowest  $L^*$ ,  $a^*$ , and  $b^*$  values of all (Fig. 3).

#### p-XRF

The component results for black, white, and red pigments used in pottery towers are shown in Fig. 4. The main elements detected through p-XRF in the black pigment were iron (Fe), calcium (Ca), potassium (K), and sulfur (S); other trace elements were hardly detected. The elements mainly detected in white pigments are Ca, S, and Fe. In the case of red pigment, the elements S, Ca, mercury (Hg), and Fe were detected. The S element was detected in a relatively higher degree than other elements, and Hg and Fe were detected in trace amounts. Based on these results for the elements Ca in the white pigment and S

and Hg in the red one, they can be presumed to be the main ingredients of each specific color. The p-XRF of the black pigment did not identify a chromophoric chemical element responsible for its color.

As shown in Fig. 4, Fe, Ca, K, and S elements were commonly detected in all pigments. This fact suggests that the pigments in the measured area were finely mixed or that components of the layer applied as a base coating on the back of the pigment layer were detected together. As X-rays penetrate beyond the surface layer of the pigment, we could analyze the components making up the base layer [8].

#### SEM-EDS

The elemental distribution of the cross-section samples was confirmed by SEM-EDS (Fig. 5). In the cross-section of the black pigment, Ca was predominant, and elements similar to clay components, such as silicon (Si), aluminum (Al), K, and Fe, were detected under the pigment layer. In the white pigment, Ca and magnesium (Mg) were present in the upper layer, and Si, Al, K, and Fe in the lower one, as was the case of the black pigment.

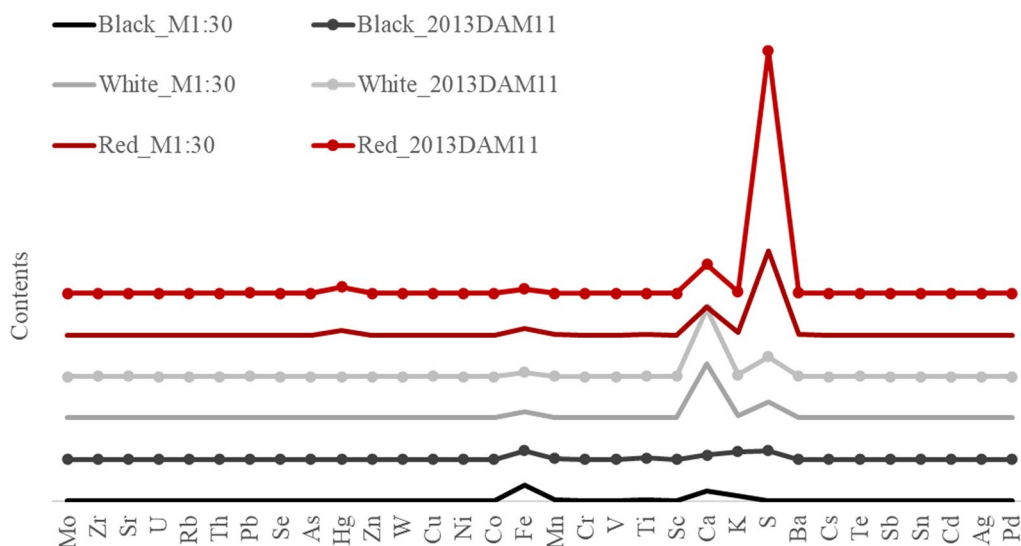


**Fig. 4** Content of elements using p-XRF in the pigments from the pottery towers (A black; B white; C red pigment, unit: ppm; Black line: DAM1-30; Gray line: DAM11-37)

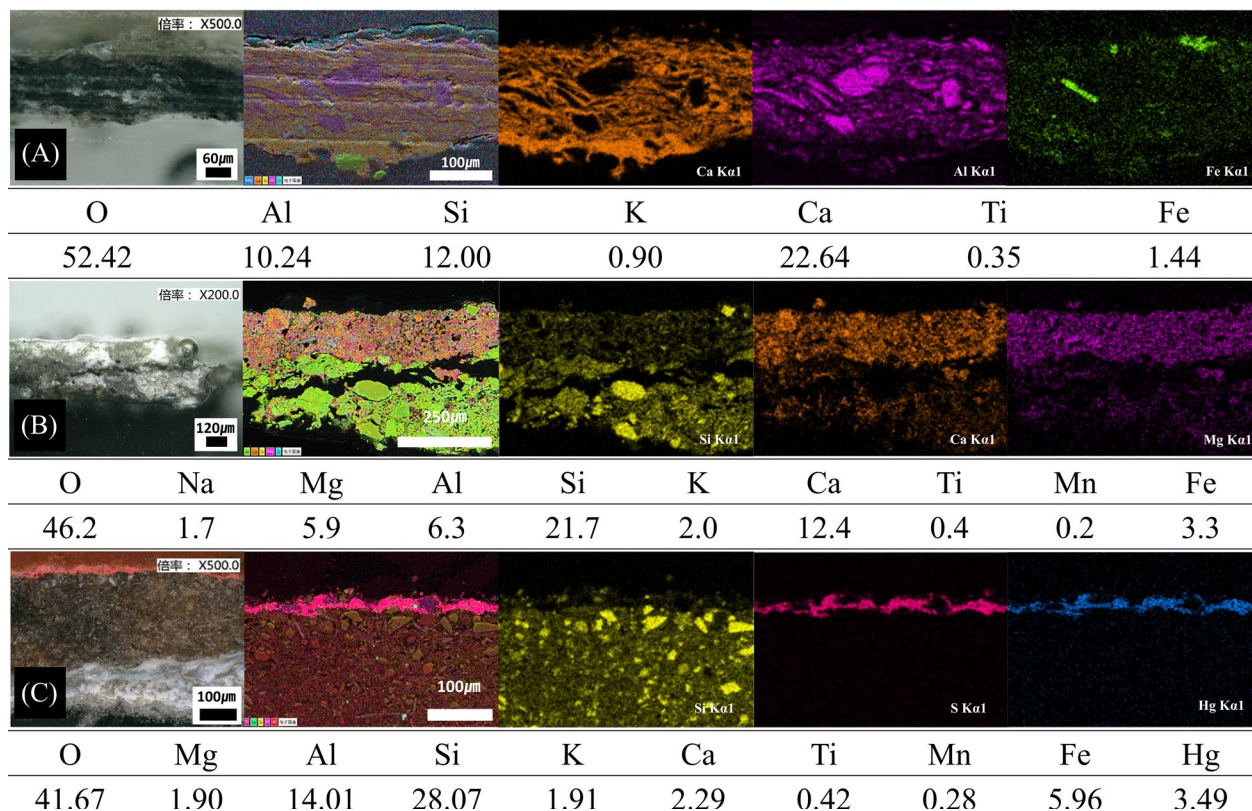


**Fig. 5** Results of the SEM–EDS mapping analysis of black (A), white (B), and red (C) pigments

Ca component was widely distributed all throughout the black one and abundantly distributed in the upper layer of the white pigment sample. The red pigment had a

thin layer where approximately 27 μm of Hg and S were detected on the surface and a lump of widely distributed Si in the lower part.

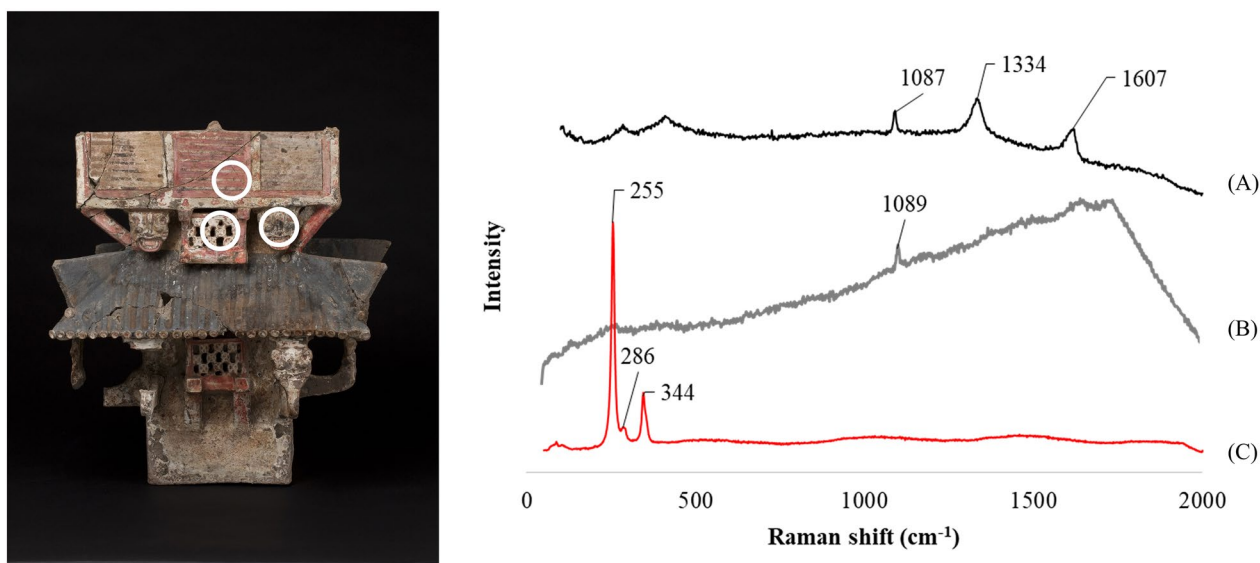


**Fig. 6** Raman spectra of pigment. A: black + white (638 nm), B: white (532 nm), C: red pigment (785 nm). The white circles in the left picture are the measurement locations

### Raman spectroscopy

Figure 6A shows the five main peaks of the Raman spectrum in the form of a mixture of white and black pigments. For convenience, the Raman spectrum was divided into two parts. These were (I) a 1200–100  $\text{cm}^{-1}$  region attributable to calcite, and (II) a 1700–1300  $\text{cm}^{-1}$  region due to carbon black. In the (I) region, the  $\nu_1$  band at 1089  $\text{cm}^{-1}$  due to symmetric stretching of the  $(\text{CO}_3)^{2-}$  group, and the  $\nu_4$  band due to the in-plane bending mode were observed at 725  $\text{cm}^{-1}$ . The  $\nu_{13}$  band attributed to lattice translation of the external vibration of the  $(\text{CO}_3)^{2-}$  group was observed around 285  $\text{cm}^{-1}$ ; it was identified as calcite due to these bands [9]. In addition, in the Raman spectrum of the region (II), two main peaks were observed: a peak at 1337  $\text{cm}^{-1}$  in the band between 1300  $\text{cm}^{-1}$  and 1400  $\text{cm}^{-1}$ , and a peak at 1617  $\text{cm}^{-1}$  in the band between 1550  $\text{cm}^{-1}$  and 1620  $\text{cm}^{-1}$ . These two bands show the wide G and D1 bands characteristic of carbon black, representing amorphous carbon particles [10–13].

In Fig. 6B, the representative 1089  $\text{cm}^{-1}$  ( $\nu_1$ ) strong peak of calcite was detected; the weak peak at 281  $\text{cm}^{-1}$ , caused by external vibration of the  $\text{CO}_3$  group including the group's translational vibration, was found and identified as calcite. The red pigment (Fig. 6C) showed a characteristic peak of cinnabar. A strong band at 254  $\text{cm}^{-1}$  was attributed to the totally symmetric A1 vibration and the 285, 343  $\text{cm}^{-1}$  bands were peaks due to degenerate E vibrations.

### Crystal optical properties, and particle shape and size

Figure 7 presents a fragment surface and the shape of the pigment in pottery towers evidenced through SEM. In the case of black pigment (Fig. 7A, B), it was difficult to identify a single particle, but it was confirmed that several spherical single particles formed the agglomeration. There was no color difference between the plane polarized light (PPL) and cross-polarized light (XPL) through observation under a polarized light microscope (Fig. 7C, D) [14]. The black pigment was confirmed at a minimum of 0.8  $\mu\text{m}$  to a maximum of 3.1  $\mu\text{m}$  in the case of single particles, and the size of the agglomerated pigment was 55  $\mu\text{m}$  or more. The average particle size value was  $1.9 \pm 0.1 \mu\text{m}$ , and the standard error value was low because it had a relatively spherical shape.

Most white pigments (Fig. 7E, F) were irregular in shape, in the form of rhombic, and only the surface was plate-shaped. The white pigment was observed in a smooth form, but upon closer look, a crystal structure of a three-dimensional rhomboid shape was confirmed (Fig. 7G, H) [15]. This characteristic of rhombic form has a strong effect on the milling process due to the cleavage characteristics of calcite. The anisotropic characteristics appear and particle distribution is very wide due to this cleavage. It is reported that this splitting characteristic is rarely seen in microsynthetic crystals, and it is believed to have been influenced by the milling process when manufacturing pigments for pottery towers. [16]. Lamellar twins, characteristic of calcite crystallography, were confirmed at the top and bottom of the particle seen in XPL picture (Fig. 7H). This is the most significant feature

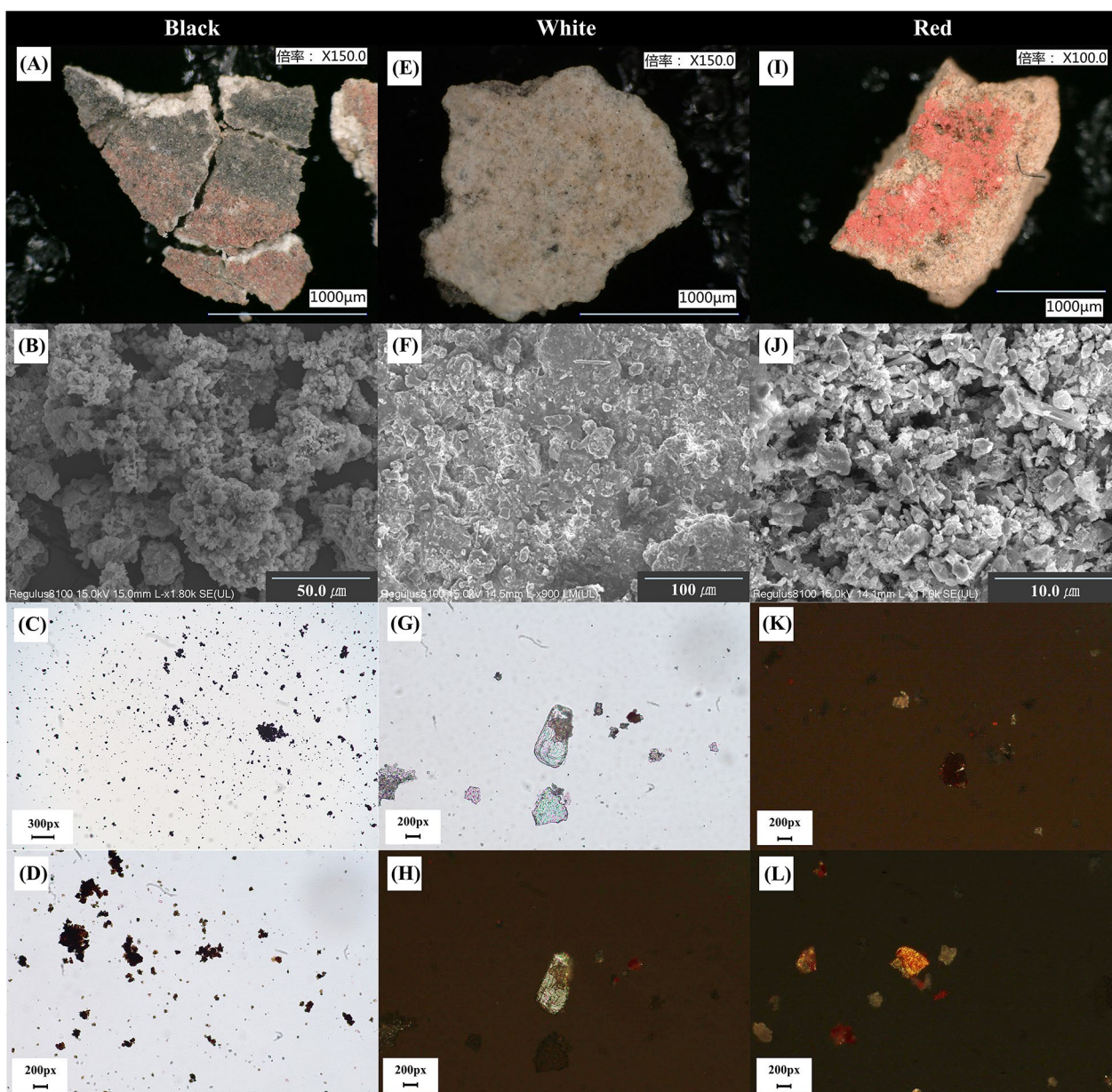


**Fig. 7** Observation images of pottery tower fragments for three types of pigments. The top row presents an optical microscopic image of the three types of pigments, the middle row SEM images, and the bottom row polarized-light microscopic images (A DAM11-37, E DAM1-30, I DAM15-71, B, F, J SEM image, C, D, G PPL; H, K, L XPL)

of calcite having different crystallographic directions. In the case of the white pigment, the minimum diameter was 35.5  $\mu\text{m}$  and the maximum was 448.4  $\mu\text{m}$ . The average value was confirmed at  $144.9 \pm 17 \mu\text{m}$ , but the error value was large because the particle was not spherical in shape but a three-dimensional rhomboid crystal.

Cinnabar has been reported to have various particle shapes [17]. The cinnabar observed in this study had a smooth surface and very small amounts of angular

prismatic crystals were found. Most of them were irregular in shape, with rough edges, (Fig. 7I, J) [17, 18]. Moreover, the particles showed pleochroism ranging from pale to deep orange-red under plane-polarized light. In Fig. 7K, L, there are colorless stripes between the large particles in the middle of the figure; the presence of these impurities is most likely characteristic of pigments derived from natural minerals.

Extant literature recounts a way to artificially produce cinnabar dating from at least the second century BC [19]. In previous research, SEM–EDS and X-ray diffraction (XRD) analysis results could not distinguish between natural and artificially-made pigments. However, they can be differentiated by their particle shape and size. In natural mineral cinnabar, the size of the pigment is not uniform and the edges are broken due to milling, while artificially-made pigments are small and uniform and tend to cluster. The particle shape of the red pigment revealed by this study is similar to that of the natural mineral cinnabar. In support of this, since the amount of pigment obtained from artifacts is remarkably small, information on the cinnabar particle size is scarce in existing literature, the average particle size of cinnabar is 37.725  $\mu\text{m}$ , and the vermilion is said to be fairly uniform, less than 1–3  $\mu\text{m}$ ; therefore, we can infer that natural mineral stone was processed and used. The minimum diameter of the red pigment was 36  $\mu\text{m}$  and the maximum 206  $\mu\text{m}$ , while the average diameter value was confirmed as  $83 \pm 6 \mu\text{m}$ .

As shown in Table 1, the white and red pigments were easily identified only by p-XRF and SEM–EDS analysis. As a result of p-XRF analysis of the red pigment, it was confirmed that the S element tended to be more present than the Hg element. When considering all results comprehensively (SEM–EDS, Raman spectroscopy, and polarizing microscope analysis), the red pigment could be identified as cinnabar composed of Hg and S. However, in the case of the black pigment, only elements similar to clay components were detected through the p-XRF and SEM–EDS analysis, and no elements capable of producing a black color were found. Consequently, we confirmed carbon as the main characteristic of this black pigment through Raman analysis.

#### Coloring technique

Macroscopy and infrared cameras were used to confirm how the pigments were applied to the pottery towers.

The white part, which is the background, was colored entirely using white pigment immediately after manufacturing (Fig. 8B). Special parts, such as doors, crossbeams, and pillars, were expressed with red and black pigments. White was applied as the base coating, black was applied on contours and streaks, and red on the surface (Fig. 8A). We presumed that the surface was made uniform and smooth using white pigment with a relatively constant pigment particle size, and the base layer was painted brightly and evenly in red and black. No other baselines or sketches were confirmed through an infrared camera (Fig. 8D, F). In China, white and red are the colors used for funerals. White represents death and yin energy, and red represents life and yang energy [20]. This coloration is specific to pottery towers, which are funeral objects and represent the burial ritual and art of the Han Dynasty in China.

#### Conclusion

This study documents the process of identifying the types of black, white, and red pigments painted on pottery towers excavated from the Daqu Tomb in Beijing, comparing and analyzing particle shapes and sizes.

The chromophoric chemical compounds were identified as carbon black, calcite white, and cinnabar red. The three types of pigments had micromorphological characteristics consistent with elemental analysis. The black pigment had a spherical single particle shape. Raman analysis was more suitable to confirm molecular fingerprints than using equipment such as p-XRF and SEM–EDS for the black pigment. In particular, through micromorphological observation of the pigments, it was possible to predict the milling process for white pigments and the manufacturing process for red pigments made of natural mineral pigments.

The white pigment was identified as calcite due to its rhombic structure and multi-twin characteristics. It can be assumed that there was an artificial milling process

**Table 1** Composition of ancient pigments through multi-analysis

Color	Sample	p-XRF	SEM–EDS	Raman ( $\text{cm}^{-1}$ )	Chemical formula
Black	DAM1-30	Fe > Ca > K		1335, 1617	C (carbon black)
	DAM11-38				
	DAM11-30	Fe > K > Ca	O > Ca > Si > Al		
	DAM11-37		O > Mn > C > Fe		
White	DAM1-30	Ca > S > Fe			CaCO <sub>3</sub> (calcite)
	DAM28			1089	
	DAM11-38				
	DAM11-30	Ca > S > Fe	O > Si > Ca		
Red	DAM1-30	S > Ca > Fe > Hg			HgS (cinnabar)
	DAM11-30	S > Ca > Hg			
	DAM15-71		Hg > S > O	256, 281, 344	

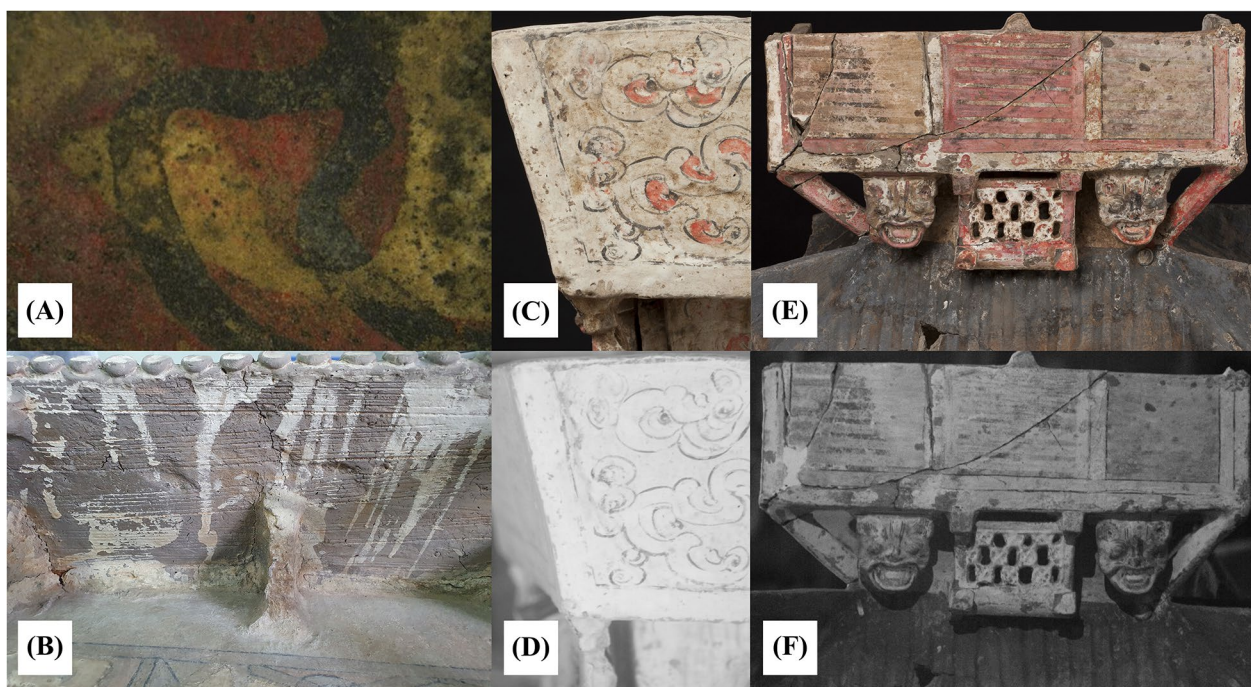


**Fig. 8** Macroscopy (A, B, C, E) and infrared camera images (D, F) of the coloring techniques used in pottery towers

leading to the rhombic structure of the white pigment. The red pigment had evidence of being manufactured from natural mineral ore, which had a wide range of particle sizes, transparent crystals between the particles, and the shape of particles with angular edges.

This study provides important information on the ancient pigments used in the Han Dynasty, and very useful basic data for repairing and restoring traditional oriental paintings and colored cultural items using pigments in the same original way.

#### Acknowledgements

The authors thank SeongWu Mun of the National Research Institute of Cultural Heritage in Korea, who discussed some of the research results with us.

#### Author contributions

IHG supervised and conducted all experiments for the article, interpreted the data and prepared the draft and final manuscripts along with XH. JQW prepared the materials and conducted experiments. NTL provided samples and internal research data. HG interpreted the analysis results and prepared the final manuscript.

#### Funding

This research was conducted as part of the China Ministry of Science and Technology project in 2021 (Foreign Youth Talent Program, QN2021105001L).

#### Availability of data and materials

All generated or analyzed data are included in this published article.

#### Declarations

#### Competing interests

The authors declare that they have no competing interests.

Received: 30 January 2023 Accepted: 19 September 2023

Published online: 26 October 2023

#### References

1. Beijing Institute of Cultural Heritage. Research on the science and technology of Han Dynasty painted pottery buildings in the Yongding River Cultural Belt of Xishan (Some excerpts from internal research report data). Beijing Municipal Bureau of Cultural Heritage Key Research Base, University of Science and Technology Beijing; 2021 (in Chinese).
2. Han DJ. An essay on the causes of the decline of Nubang architecture in the Han Dynasty/earthquake impact theory. *J Archit Hist.* 2002;11(2):146–9 (in Korean).
3. Shin IJ. A study on molded pottery in the Three Kingdoms period. *Culture.* 2001;5(5):93–133 (in Korean).
4. Chen G. Color research of Han Dynasty's tomb mural. College of Fine Arts, Dissertation. Shanghai University, Shanghai; 2015 (in Chinese).
5. Rong B, Lan DS, Wang L, Zhu ZY, Li B, Wang CY. Study and analysis of the pigment of polychromy pottery during Han Dynasty excavated in Xian Yang. *Painted Cultural Relics Protection Technology*; 2009.
6. Jin PJ, Lu WJ, Wang CS. Research on the red pigment unearthed from Han Dynasty Tombs in Dafangying Reservoir, North Gate of Hefei. *Culture.* 2007;3(197):58–61 (in Chinese).
7. Thomason JL, Carruthers J, Kelly J, Johnson G. Fibre cross-section determination and variability in sisal and flax and its effects. *J Compos Sci Technol.* 2011;71:1008–15.
8. Chun YG, Lee CH. Pigment analysis for wall paintings according to verification of penetration depth for X-ray: Ssanggyesa Daeungjeon (Main Hall of Ssanggyesa Temple) Nonsan. *J Conserv Sci.* 2011;27(3):269–76 (in Korean).
9. Sun JM, Wua ZG, Cheng HF, Zhang ZJ, Frost RL. Raman spectroscopic comparison of calcite and dolomite. *SAA.* 2014;117:158–62.

10. Hernanz A, Bratu I, Marutoiu OF, Marutoiu C. Micro-Raman spectroscopic investigation of external wall paintings from St. Dumitru's Church, Suceava, Romania. *Anal Bioanal Chem.* 2008;392:263–8.
11. Coccato A, Jehlicka J, Moens L, Vandenberghe P. Raman spectroscopy for the investigation of carbon-based black pigments. *J Raman Spectrosc.* 2015;46:1003–15.
12. Jawhari T, Roid A, Casado J. Raman spectroscopic characterization of some commercially available carbon black materials. *Carbon.* 1995;33(11):1561–5.
13. Scheuermann W, Ritter GJ. Raman spectra of cinnabar (HgS), Realgar (As<sub>4</sub>S<sub>4</sub>) and Orpiment (As<sub>2</sub>S<sub>3</sub>). *J Phys Sci.* 1969;24a:408–11.
14. Nam TG, Shin SJ, Park WK, Kim BR. Analysis of characterization on ancient ink stick. *J Conserv Sci.* 2012;28(2):165–73 (in Korean).
15. Manzine Costa LM, Molina de Olyveira G, Salomão R. Precipitated calcium carbonate nano-microparticles: applications in drug delivery. *Adv Tissue Eng Regen Med.* 2017;3(2):336–40.
16. Eastaugh N, Walsh V, Chaplin T, Siddall R. *Pigment compendium, a dictionary and optical microscopy of historical pigments.* London: Routledge; 2017.
17. Yoo YM, Han MS, Lee JJ. Species and characteristics of particles for traditional red and green pigments used in temples. *J Conserv Sci.* 2014;30(4):365–72 (in Korean).
18. Li MY. *Research on pigments for decorative polychrome painting in official handicraft regulations and precedents of Qing Dynasty.* Dissertation, Tsinghua University, Beijing; 2019 (in Chinese).
19. Wo JY. *Research of pigments in the pre-Qin and Han Dynasties.* Dissertation. Tianjing University of Architecture, Tianjing; 2001 (in Chinese).
20. Chen SL. *Architectural features and cultural research reflected by Ming artifacts in the Wei, Jin, Southern and Northern Dynasties.* Dissertation. Xian University of Architecture and Technology, Xian; 2014 (in Chinese).

### Publisher's Note

Springer Nature remains neutral with regard to jurisdictional claims in published maps and institutional affiliations.

Submit your manuscript to a SpringerOpen® journal and benefit from:

- Convenient online submission
- Rigorous peer review
- Open access: articles freely available online
- High visibility within the field
- Retaining the copyright to your article

---

Submit your next manuscript at ► [springeropen.com](https://www.springeropen.com)

---